Uncoupling and endocytosis of 5-hydroxytryptamine 4 receptors. Distinct molecular events with different GRK2 requirements.

Gaël Barthet, Florence Gaven, Bérénice Framery, Katsuhiro Shinjo, Takaaki Nakamura, Sylvie Claeysen, Joël Bockaert, Aline Dumuis

HAL Id: inserm-00092206

https://inserm.hal.science/inserm-00092206

Submitted on 20 Feb 2020

Uncoupling and Endocytosis of 5-Hydroxytryptamine 4 Receptors

DISTINCT MOLECULAR EVENTS WITH DIFFERENT GRK2 REQUIREMENTS*[S]

Gaël Barthet‡, Florence Gaven‡, Bérénice Framery‡, Katsuhiro Shinjo§, Takaaki Nakamura§, Sylvie Claeysen‡, Joël Bockaert‡¶, and Aline Dumuis‡

From ‡CNRS UMR5203, Montpellier, F-34094 France, INSERM, U661, Montpellier, F-34094 France, Université Montpellier I, Montpellier, F-34094 France, Université Montpellier II, Montpellier, F-34094 France, Institut de Génomique Fonctionnelle, 141 Rue de la Cardonille, Montpellier F-34094 Cedex 5, France, and §Nagoya Laboratories, Pfizer Japan Incorporated, 5-2 Taketoyo, Aichi 470-2393, Japan

The 5-hydroxytryptamine type 4 receptors (5-HT$_4$Rs) are involved in memory, cognition, feeding, respiratory control, and gastrointestinal motility through activation of a G$_s$/cAMP pathway. We have shown that 5-HT$_4$R undergoes rapid and profound homologous uncoupling in neurons. However, no significant uncoupling was observed in COS-7 or HEK293 cells, which expressed either no or a weak concentration of GRK2, respectively. High expression of GRK2 in neurons is likely to be the reason for this difference because overexpression of GRK2 in COS-7 and HEK293 cells reproduced rapid and profound uncoupling of 5-HT$_4$R. We have also shown, for the first time, that GRK2 requirements for uncoupling and endocytosis were very different. Indeed, β-arrestin/dynamin-dependent endocytosis was observed in HEK293 cells without any need of GRK2 overexpression. In addition to this difference, uncoupling and β-arrestin/dynamin-dependent endocytosis were mediated through distinct mechanisms. Neither uncoupling nor β-arrestin/dynamin-dependent endocytosis required the serine and threonine residues localized within the specific C-terminal domains of the 5-HT$_4$R splice variants. In contrast, a cluster of serines and threonines, common to all variants, was an absolute requirement for β-arrestin/dynamin-dependent receptor endocytosis, but not for receptor uncoupling. Furthermore, β-arrestin/dynamin-dependent endocytosis and uncoupling were dependent on and independent of GRK2 kinase activity, respectively. These results clearly demonstrate that the uncoupling and endocytosis of 5-HT$_4$R require different GRK2 concentrations and involve distinct molecular events.

5-Hydroxytryptamine 4 receptors (5-HT$_4$Rs)[1] are widely expressed in the brain and at the periphery (1, 2). They are implicated in important physiological functions such as memory, cognition, feeding, respiratory control, and gastrointestinal motility (3–6). Among the G protein-coupled receptor (GPCR) genes, the 5-HT$_4$R gene is one of the largest (700 kb) (7, 8). To date, nine variants have been cloned in human, four in mouse, and three in rat. All of these variants differ at their C termini after a single position (Leu[358]). They share different sets of Ser and Thr residues in their specific domains and a common cluster of six Ser and Thr residues upstream of the splice site. All are putative sites for G protein receptor kinase (GRK)-mediated phosphorylation. 5-HT$_4$Rs are coupled to the G$_s$/cAMP/protein kinase A pathway (9). Other signal transduction pathways have also been reported, but mainly in heterologous transfected cells (2, 10, 11).

Twelve years ago, before the 5-HT$_4$R was cloned, we reported that activation of 5-HT$_4$R in colliculus neurons is followed by strong and rapid homologous desensitization unaffected by cAMP (12). Since this early work, very little additional information has been learned about the molecular mechanisms involved in the desensitization of this important receptor. Recently, Ponimaskin *et al.* (13) showed that 5-HT$_{4(a)}$Rs are phosphorylated when heterologously expressed in insect cells. This phosphorylation is modulated by palmitoylation of Cys residues present in the C-terminal domain and is unrelated to the weak desensitization observed when the receptor is transfected in COS-7 cells.

GPCR activity represents a coordinated balance between molecular mechanisms governing receptor signaling, desensitization, and resensitization (14). The homologous desensitization of GPCR signaling is a multistep process, classically described by four main events (15–20). In the first step, GPCR is uncoupled from the G proteins following stimulation of the receptor by the agonist, resulting in attenuation of the primary response (*i.e.* second messenger production or channel regulation). In most cases, this process, often called "desensitization," involves GRKs. However, in some cases, the kinase activity of GRKs is not required (21–25). Receptor/G protein uncoupling is due not only to phosphorylation of the receptor *per se*, but also to binding of β-arrestins (26–28). The second step is "endocytosis" of the receptor (29), which is often, but not always, β-arrestin-dependent (17, 30). The molecular characteristics involved in the interaction between the receptor and β-arrestin determine the particularities of endocytosis, intracellular trafficking, recycling, and resensitization (third step) or degradation (fourth step; also called "down-regulation") (20, 31–34).

GPCRs have been divided into two classes based on their

[S] The on-line version of this article (available at http://www.jbc.org) contains Supplemental Table 1.

¶ To whom correspondence should be addressed: Dépt. de Neurobiologie, Inst. de Génomique Fonctionnelle, 141 Rue de la Cardonille, Montpellier F-34094 Cedex 5, France. Tel.: 33-4-6714-2930; Fax: 33-4-6714-2910 or 33-4-6754-2432; E-mail: joel.bockaert@igf.cnrs.fr.

[1] The abbreviations used are: 5-HT$_4$Rs, 5-hydroxytryptamine 4 receptors; GPCR, G protein-coupled receptor; GRK, G protein-coupled receptor kinase; HEK, human embryonic kidney; YFP, yellow fluorescent protein; HA, hemagglutinin; DMEM, Dulbecco's modified Eagle's medium; ELISA, enzyme-linked immunosorbent assay; 5-HT, 5-hydroxytryptamine; WT, wild-type.

This paper is available on line at http://www.jbc.org

aptitude to bind β-arrestin (33). Class A receptors (*e.g.* μ-opioid, β$_2$- and α$_{1B}$-adrenergic, and dopamine D$_1$ receptors) are defined by the presence of scattered Ser/Thr residues, rapid dissociation of arrestins, and rapid recycling back to the cell surface. Class B receptors (*e.g.* substance P, angiotensin 1a, and vasopressin-2 receptors) are defined by the presence of clustered Ser/Thr residues, formation of a stable complex with arrestins, and predominant targeting to lysosomes for degradation (down-regulation) (33). Although this model may be applied to many GPCR/arrestin interactions, there are exceptions. For example, a recent study by Tulipano *et al.* (35) showed that somatostatin 2a receptors belonging to class B, characterized by stable association with β-arrestin, are rapidly resensitized and recycled back to the plasma membrane, unlike other class B receptors.

Molecular processes for GPCR desensitization are pleiotropic and generally receptor-specific. Understandably, studies have been performed in heterologous cell lines because, unlike neuronal cultures, these systems are easily transfected and analyzed in molecular and biochemical terms. However, as recently reviewed, the signaling pathways of a given receptor are highly dependent on the cell line or even the subclone used (36, 37). Because the final goal is, of course, to understand what occurs in native tissues, our first goal was to compare the desensitization profile of 5-HT$_4$Rs obtained in colliculus neurons *versus* heterologous cell lines. A marked difference was found; in colliculus neurons, uncoupling was rapid and intense, whereas it was slow and weak in COS-7 and HEK293 cells. We found that colliculus neurons expressed only GRK2, but at a high density. Overexpression of GRK2 in COS-7 or HEK293 cells was sufficient to observe rapid and marked uncoupling of 5-HT$_4$Rs, as seen in colliculus neurons. This uncoupling was not dependent on the presence of Ser and Thr residues at the specific C-terminal domains, and full uncoupling could be obtained by overexpressing the kinase-deficient GRK2(K220R) mutant. The molecular events involved in the uncoupling step were clearly different from those implicated in endocytosis. Indeed, 5-HT$_4$R endocytosis could be obtained in HEK293 cells without any overexpression of GRK2. This β-arrestin/dynamin-dependent endocytosis required the presence of the cluster of serines and threonines common to all variants and the kinase activity of GRK2. The kinase-deficient GRK2 mutant inhibited β-arrestin-dependent endocytosis, but promoted β-arrestin-independent endocytosis. Thus, desensitization can be further broken down into two independent molecular events, uncoupling and endocytosis.

EXPERIMENTAL PROCEDURES

Plasmids—Plasmids pRK5-GRK2 and pRK5-DN-GRK2(K220R) (where DN is dominant-negative) were kindly provided by Dr. S. Cotecchia (Faculté de Médecine, Université de Lausanne, Lausanne, Switzerland). Plasmid pRK5-GRK5 (constructed in the laboratory of Dr. R. J. Lefkowitz (Duke University Medical Center, Durham, NC)) was kindly provided by Dr. J. Pitcher (University College, London, UK). Plasmids pcDNA3.1-GRK4, pcDNA3.1-GRK6, and pcDNA3.1-β-arrestin-2-YFP were generously provided by Dr. M. Bouvier (University of Montreal, Montreal, Canada). pcDNA3-DN-β-arrestin-(319–418) was generated in the laboratory of Dr. J. L. Benovic as described (38) and kindly provided by Dr. M. Bouvier. Plasmid pcDNA3.1-DN-dynamin(K44A) (generated by Dr. M. A. McNiven (Mayo Cancer Center, Guggenheim, Rochester, MN)) (39) was kindly provided by Dr. C. Lamaze (Institut Curie, Paris, France).

Construction of Tagged 5-HT$_4$R cDNAs—The c-Myc-tagged 5-HT$_4$R and Rho-tagged 5-HT$_4$R constructs were described previously (10, 40). Hemagglutinin (HA)-tagged 5-HT$_4$R cDNAs in pRK5 were generated by fusing the sequence of the HA epitope (YPYDVPDYA) to a cleavable signal peptide (MVLLLILSVLLLKEDVRGSAQS) derived from the metabotropic glutamate type 5 receptor. This sequence was inserted into the pRK5 vector using XbaI and MluI restriction sites. Then, full-length mouse 5-HT$_{4(a)}$R, 5-HT$_{4(b)}$R, 5-HT$_{4(e)}$R, and 5-HT$_{4(f)}$R cDNAs were sub-

cloned in-frame using MluI and HindIII.

Construction of Truncated and Mutated 5-HT$_{4(a)}$R cDNAs—Truncated receptor constructs were described previously (10). Briefly, constructs Δ346 and Δ358 were obtained by inserting a stop codon after residue 327, 346, or 358 in the 5-HT$_{4(a)}$R cDNA sequence using the QuikChange site-directed mutagenesis kit (Stratagene, Amsterdam, The Netherlands). The same kit was used to replace Ser or Thr residues between positions 347 and 355 with alanine residues to generate the Δ358Ala construct.

Antibodies—Anti-GRK4/5/6 monoclonal antibody was generated in the laboratory of Dr. R. J. Lefkowitz (41), who generously provided it. Anti-GRK2/3 polyclonal antibody was purchased from Tebu, Le Perray en Yvelines, France. Rabbit anti-HA antibody SG77 was purchased from Cliniscience, Montrouge, France. Mouse anti-c-Myc antibody 9E10 was a gift from Dr. B. Mouillac (Institut de Génomique Fonctionnelle, Montpellier, France). Mouse anti-Rho tag antibody was provided by Dr. S. Costagliola (Institut de Recherche en Biologie Humaine et Nucléaire, Brussels, Belgium) (40). Alexa Fluor 594-labeled secondary antibody was purchased from Invitrogen, Cergy-Pontoise, France. Horseradish peroxidase-conjugated anti-rabbit and anti-mouse antibodies were from Amersham Biosciences (Orsay, France).

RNA Preparation and Real-time Quantitative Reverse Transcription-PCR—Total RNA was extracted from colliculus neurons in primary culture using TRIzol (Invitrogen) and treated with DNase I from a DNA-free™ kit (Ambion, Cambs, UK) according to the manufacturer's instructions. RNA was then used to perform two-step reverse transcription-PCR. Briefly, 1 μg of DNA-free total RNA was reverse-transcribed using 200 units of Moloney murine leukemia virus reverse transcriptase (Invitrogen) in the presence of 2.5 μM random primers and 0.5 mM dNTP. The resulting cDNA (20 ng) was used as a template for real-time PCR using ABI PRISM 7000 with SYBR® Green PCR Master Mix, Applera, Courtaboeuf, France. Standard curves were performed for each 5-HT$_4$R variant by serial dilutions of the corresponding cDNA. Primers were designed with Primer Express™ software (Applied Biosystems). The sequences of all primers used are provided in Supplemental Table 1. PCR was performed in 10 μl in the presence of 300 nM specific primers. Thermal cycling parameters were 2 min at 50 °C and 10 min at 95 °C, followed by 40 cycles for 15 s at 95 °C and 1 min at 60 °C. Data were analyzed with ABI PRISM 7000 SDS software, and the threshold cycle (C_t) was calculated from each amplification plot. Standard curves (C_t value (*y*) *versus* log copy number (*x*)) were used to calculate the relative input amount of mRNA for each variant based on the C_t value (42). Results are expressed as a percentage of the most abundant variant (5-HT$_{4(b)}$R). Data are the means ± S.D. of duplicate determinations and are representative of three independent experiments.

Cell Cultures and Transfection—Primary cultures of colliculus neurons were prepared as described previously (43). Briefly, cells dissociated from the colliculi of 14–15-day-old Swiss mouse embryos were plated in serum-free medium in 12-well culture dishes (0.8×10^6 cells/ml, 1 ml/dish). Cultures were maintained for 6 days at 37 °C in a humidified atmosphere of 5% CO$_2$, 95% H$_2$O, and air. Colliculus neurons were nucleofected using a mouse neuron Nucleofector™ kit (Amaxa Biosystems, Koeln, Germany). One Nucleofection sample contains 5×10^6 cells, 3 μg of HA-tagged or Rho-tagged 5-HT$_4$R cDNA in pRK5, and 100 μl of mouse neuron Nucleofector solution according to the manufacturer's instructions. COS-7 and HEK293 cells were grown in Dulbecco's modified Eagle's medium (DMEM) supplemented with 10% dialyzed fetal calf serum and antibiotics. They were transfected to 60–70% confluence by electroporation as described previously (10). Colliculus neurons and transfected COS-7 and HEK293 cells were processed for subsequent experiments: desensitization, immunofluorescence, Western blotting, and cell-surface enzyme-linked immunosorbent assay (ELISA).

Determination of cAMP Production in Transfected Cells—COS-7 or HEK293 cells were transfected with the appropriate cDNA and plated in 24-well plates (70,000 cells/well). Twenty-four hours post-transfection, a 5-min stimulation with the appropriate concentrations of 5-hydroxytryptamine (5-HT), 0.1 mM L-ascorbic acid, and 0.1 mM Ro 20-1724 (phosphodiesterase inhibitor) was performed at 37 °C in 250 μl of HEPES-buffered saline (20 mM HEPES, 150 mM NaCl, 4.2 mM KCl, 0.9 mM CaCl$_2$, 0.5 mM MgCl$_2$, 0.1% glucose, and 0.1% bovine serum albumin). The same volume of Triton X-100 (0.1%) was added to stop the reaction, and the cells were incubated for 30 min at 37 °C. Quantification of cAMP production was performed by HTRF™ (homogenous time-resolved fluorescence) using a cAMP dynamic kit (CIS Biointernational, Bagnols-sur-Cèze, France) according to the manufacturer's instructions.

Uncoupling of 5-HT$_4$R-stimulated cAMP Production in Colliculus Neurons—To analyze receptor desensitization, neurons endogenously expressing 5-HT$_4$Rs (prepared as described above) were preincubated with 10 μM 5-HT for the indicated time periods (0–2 h). After three washes with culture medium, cAMP accumulation was started by addition of culture medium containing 5-HT (30 μM), isobutylmethylxanthine (1 mM), and forskolin (0.1 μM), and the accumulation was measured for 5 min. Quantification of cAMP production was performed as described under "Determination of cAMP Production in Transfected Cells."

Uncoupling of 5-HT$_4$R-stimulated cAMP Production in the Heterologous System—COS-7 or HEK293 cells were transfected with the indicated 5-HT$_4$R construct (wild-type (WT) or mutant) either alone or in combination with GRKs as indicated in the figure legends. Cells were seeded at 0.5×10^6/well on a 24-well plate 1 day prior to the experiment. To analyze receptor uncoupling, cells expressing 5-HT$_4$R in the presence or absence of GRKs were first preincubated with 5-HT (10 μM) for different time periods (uncoupling period). Subsequently, the cells were washed three times with HEPES-buffered saline, and cAMP accumulation was initiated by addition of HEPES-buffered saline containing 5-HT (10 μM) with L-ascorbic acid (0.1 mM) and the phosphodiesterase inhibitor Ro 20-1724 (0.1 mM). The accumulation was measured for 5 min. Quantification of cAMP production was performed as described under "Determination of cAMP Production in Transfected Cells."

Intact Cell 5-HT$_4$R Phosphorylation—To measure phosphorylation of Rho-tagged 5-HT$_4$R in intact cells, transiently transfected COS-7 cells were plated at a density of 5×10^6 cells/dish on 100-mm dishes. The next day, the cells were washed with serum- and phosphate-free DMEM and then labeled with 150 μCi/ml [^{32}P]orthophosphate for 90 min at 37 °C. Labeled cells were stimulated or not with 10 μM 5-HT for 10 min as indicated in the figure legends. Subsequently, cells were placed on ice and washed with ice-cold phosphate-buffered saline and then solubilized in 1 ml of radioimmune precipitation assay buffer containing 50 mM Tris-HCl (pH 7.4), 150 mM NaCl, 2.5 mM EDTA, 1% Nonidet P-40, 0.5% sodium deoxycholate, 0.1% SDS, 1 mM sodium orthovanadate, 10 mM sodium fluoride, 1 mM disodium pyrophosphate, and a protease inhibitor mixture (Roche Applied Science). The samples were cleared by centrifugation for 5 min at 20,000 × g. Soluble proteins were incubated overnight at 4 °C with 8 μg of anti-Rho tag monoclonal antibody. Samples were incubated for 2 h at 4 °C with 50 μl of protein A-Sepharose beads (Amersham Biosciences). After washes with radioimmune precipitation assay buffer, the immunoprecipitated proteins were eluted in SDS sample buffer and resolved by 10% SDS-PAGE; the gel was dried; and ^{32}P was detected by autoradiography using Kodak BioMax MS film (PerkinElmer Life Sciences, Courtaboeuf, France).

Immunofluorescence and Confocal Microscopy—HEK293 cells were used for microscopy because of their favorable morphology for comparison of the cytoplasmic and plasma membrane distribution of proteins. Cells overexpressing YFP-tagged β-arrestin-2 or c-Myc-tagged 5-HT$_4$R were grown on poly-L-ornithine-coated glass coverslips and incubated in DMEM with 10% fetal calf serum. Thirty-four hours after transfection, cells were serum-starved overnight. To visualize c-Myc-tagged receptors, cell-surface receptors were labeled with 1 μg/ml anti-c-Myc antibody 9E10 for 2 h at 4 °C. Cells were then washed with serum-free medium and stimulated with 10 μM 5-HT in the same medium at 37 °C. Cells were washed with phosphate-buffered saline, fixed with 4% paraformaldehyde for 20 min at room temperature, and then permeabilized with 0.05% Triton X-100. Cells were incubated for 1 h at room temperature with Alexa Fluor 594-coupled goat anti-mouse antibody at 2 μg/ml. After extensive washes, the coverslips were mounted onto slides using Mowiol mounting medium. Immunofluorescence microscopy was performed using a Zeiss Axiophot 2 microscope with Zeiss ×63 1.4 numerical aperture oil immersion lenses. Excitation and emission filters for the different labeled dyes were as follow: YFP (green), $\lambda_{ex} = 450–490$ nm and $\lambda_{em} = 520$ nm; and Alexa Fluor 594 (red), $\lambda_{ex} = 546$ nm and $\lambda_{em} = 590$ nm. Analysis of endocytosis in colliculus neurons was performed with a Zeiss LSM 510 META confocal microscope. Rho-tagged 5-HT$_4$Rs were labeled with 0.5 μg/ml anti-Rho antibody. Secondary labeling was carried out with Alexa Fluor 488-conjugated antibody. Slides was excited at 488 nm with an argon laser. Series of optical sections were obtained with a step of 0.30 μm. For receptor recycling experiments, cells were washed twice with serum-free medium after stimulation. Cells were then incubated in DMEM for different times of recycling before fixation.

Immunoblotting—Proteins separated by SDS-PAGE were transferred electrophoretically onto nitrocellulose membranes (Hybond-C, Amersham Biosciences). Membranes were incubated overnight at 4 °C with primary antibody. Membranes were washed three times for 10 min

with 50 mM Tris (pH 7.4), 150 mM NaCl, and 0.2% Tween 20 containing 5% nonfat dried milk and incubated for 1 h at room temperature with secondary antibodies. Proteins were detected using a Chemiluminescence Reagent Plus kit (PerkinElmer Life Sciences).

Cell-surface ELISA—HEK293 cells were transfected with HA-tagged 5-HT$_4$R alone or in combination with GRK2, GRK2(K220R), dominant-negative β-arrestin-(319–418), or dominant-negative dynamin(K44A) as indicated in the figure legends. Cells were grown on poly-L-ornithine-coated 96-well plates in DMEM with 10% fetal calf serum. Twenty-four hours post-transfection, cells were stimulated or not with 10 μM 5-HT in serum-free medium at 37 °C. After one wash, cells were fixed with 4% (w/v) paraformaldehyde for 15 min at room temperature and blocked with phosphate-buffered saline containing 1% fetal calf serum (blocking buffer). Cells were then incubated with anti-HA antibody at 0.6 μg/ml for 30 min in the same buffer. After four washes with blocking buffer, cells were incubated with horseradish peroxidase-conjugated anti-rabbit antibody at 1 μg/ml for 30 min. After extensive washes, chromogenic substrate (SuperSignal® ELISA femto maximum sensitivity substrate, Perbio, Brebières, France) was added. Chemiluminescence was detected and quantified using a Wallac Victor2 luminescence counter. For each experiment, mock conditions corresponding to cells transfected with empty vector were included. The level of receptors at the cell surface was expressed as a percentage of the residual surface receptor relative to the maximum detected before any treatment.

Data Analysis—The dose-response curves were fitted using Graph-Pad Prism and the following equation for monophasic dose-response curves: $y = (y_{max} - y_{min})/(1 + (x/EC_{50})n_H) + y_{min}$, where EC_{50} is the concentration of the compound necessary to obtain 50% of the maximum effect and n_H is the Hill coefficient. All data represented correspond to the means ± S.E. of three independent experiments performed in triplicate. Statistical analysis was carried out with the t test using GraphPad Prism 3.0 software. p values <0.05 were considered as statistically significant.

RESULTS

The Rapid and Potent Uncoupling of 5-HT$_4$R in Colliculus Neurons Is Not Observed in the COS-7 or HEK293 Cell Line— Previous work in our laboratory revealed a rapid homologous desensitization of 5-HT$_4$R in mouse colliculus neurons (12). Indeed, preincubation of mouse colliculus neurons with 5-HT (10 μM) for different periods of time (0–60 min), called the "uncoupling period" (Fig. 1A), drastically reduced the accumulation of cAMP measured during a subsequent 5-min incubation in the presence of 5-HT (10 μM), isobutylmethylxanthine (1 mM), and forskolin (0.1 μM). After a 5-min uncoupling period, the maximum stimulation was already reduced by 62%, and after 60 min, by >90% (Fig. 1A).

In an effort to better understand the molecular mechanisms involved in this process, we first wanted to identify the relative expression levels of the various isoforms endogenously present in these neuronal cells. Four 5-HT$_4$R splice variants (5-HT$_{4(a)}$R, 5-HT$_{4(b)}$R, 5-HT$_{4(e)}$R, and 5-HT$_{4(f)}$R) have been cloned in mouse colliculus neurons (10). Using real-time quantitative reverse transcription-PCR with total colliculus neuronal mRNA, we found that three of the four splice variants were significantly expressed (5-HT$_{4(a)}$R, 5-HT$_{4(b)}$R, and 5-HT$_{4(e)}$R), as shown in Fig. 1B, with the expression of mouse 5-HT$_{4(b)}$R being the greatest.

To determine whether the potent and rapid uncoupling observed in neurons also occurs in a heterologous cell system and whether one of the splice variants specifically undergoes more rapid uncoupling, we transfected COS-7 cells with each of these variants. Interestingly, as shown in Fig. 1C, none of the splice variants were dramatically uncoupled following agonist stimulation in COS-7 cells. The time courses of desensitization were very slow, and a 60-min preincubation with 5-HT (10 μM) reduced the maximum agonist stimulation by only 20%. Similar results were obtained with HEK293 cell lines both when transiently transfected (Fig. 1D) or when stably expressing 5-HT$_4$R (data not shown). Therefore, unlike the β_2-adrenergic or dopamine D$_1$ receptor (28, 44), the 5-HT$_4$R splice variants did not undergo a rapid loss of response in these heterologous
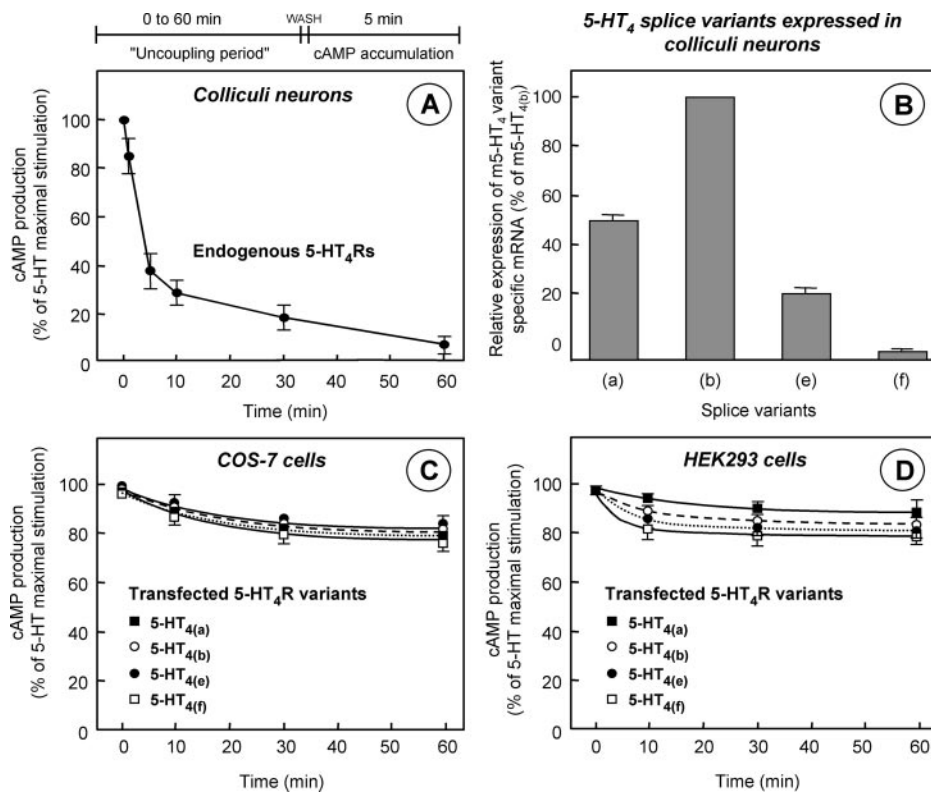
Fig. 1. **Time course of 5-HT$_4$R uncoupling in colliculus neurons and COS-7 and HEK293 cells: comparison of different 5-HT$_4$R splice variants.** Colliculus neurons (after 6 days in culture) or COS-7 or HEK293 cells (24 h after transfection) were incubated with 10 μM 5-HT for the indicated times (referred to as the uncoupling period), as shown in *A*. After three extensive washes with medium, cAMP accumulation was started by addition of medium containing phosphodiesterase inhibitor (1 mM isobutylmethylxanthine for neurons or 0.1 mM Ro 20-1724 for COS-7 and HEK293 cells) and 30 μM 5-HT as described under "Experimental Procedures." cAMP accumulation was measured for 5 min at 37 °C. Results are expressed as a percentage of the residual stimulation relative to the maximum stimulation obtained for the appropriate receptor variant. Results are the mean of three independent experiments. *A*, colliculus neurons endogenously expressing the 5-HT$_{4(a)}$R, 5-HT$_{4(b)}$R, 5-HT$_{4(e)}$R, or 5-HT$_{4(f)}$R splice variant. Basal and 5-HT-stimulated cAMP values were 35 $\pm$ 6 and 86 $\pm$ 7 pmol/well, respectively. *B*, evaluation of the expression profile of mouse (*m*) 5-HT$_4$R splice variant mRNA in colliculus neurons. mRNAs for mouse cloned variants (5-HT$_{4(a)}$R, 5-HT$_{4(b)}$R, 5-HT$_{4(e)}$R, and 5-HT$_{4(f)}$R) were quantified by real-time quantitative reverse transcription-PCR using total RNA extracted from colliculus neurons in primary culture. Standard curves (C_t value (*y*) *versus* log copy number (*x*)) were used to calculate the relative input amount of mRNA for each variant based on the C_t value. Results are expressed as a percentage of the most abundant variant (5-HT$_{4(b)}$R). *C* and *D*, COS-7 and HEK293 cells, respectively, transiently transfected with 100 ng of plasmid encoding the 5-HT$_{4(a)}$R, 5-HT$_{4(b)}$R, 5-HT$_{4(e)}$R, or 5-HT$_{4(f)}$R splice variant. In COS-7 cells, basal and 5-HT-stimulated cAMP values were 28 $\pm$ 5 and 167 $\pm$ 8 pmol/well, respectively. In HEK293 cells, basal and 5-HT-stimulated cAMP values were 4 $\pm$ 2 and 26 $\pm$ 5 pmol/well, respectively. Data are the means $\pm$ S.D. of duplicate determinations and are representative of three independent experiments.

expression systems. Obviously, some key elements of 5-HT$_4$R uncoupling were missing.

GRK2 Is Likely to Be the Kinase Involved in the Rapid and Potent Uncoupling in Colliculus Neurons—It is well known that GRKs are often an important component in receptor/G protein uncoupling process; therefore, we analyzed the nature of the endogenous GRKs expressed in colliculus neurons. We found that only GRK2 was expressed at high density, whereas GRK4/5/6 expression remained undetectable. A very low density expression of endogenous GRKs was detected in COS-7 cells (GRK3) (Fig. 2*A*) and a modest density expression in HEK293 cells (GRK2/3) (Fig. 2*C*, *inset*).

To assess whether or not 5-HT$_4$Rs can be uncoupled by any of the main GRKs, we cotransfected 5-HT$_{4(a)}$R with one of the following kinases: GRK2, GRK4, GRK5, or GRK6. Expression of either GRK4 or GRK6 failed to attenuate 5-HT$_{4(a)}$R-stimulated cAMP production, whereas GRK5 and GRK2 reduced 5-HT$_{4(a)}$R-stimulated cAMP production by 30 and 75%, respectively (Fig. 2*B*). Moreover, when GRK2 was overexpressed in COS-7 or HEK293 cells, the time course and the efficiency of 5-HT$_4$R uncoupling were very similar to those observed in colliculus neurons (Fig. 2*C*). The fact that GRK2 is highly expressed endogenously in colliculus neurons, in combination with the observation that GRK2 overexpression in heterolo-

gous systems can mimic the uncoupling profile seen in neurons, strongly implicates GRK2 as the molecule responsible for this effect.

Ser and Thr Residues Present in Specific Domains of the 5-HT$_4$R Splice Variants and in Their Common Upstream Ser/Thr Cluster Are Not Implicated in GRK2-mediated Uncoupling—To determine whether one of the splice variants specifically undergoes more rapid uncoupling, we transfected COS-7 cells with each of the four mouse splice variants that are expressed in colliculus neurons (5-HT$_{4(a)}$R, 5-HT$_{4(b)}$R, 5-HT$_{4(e)}$R, and 5-HT$_{4(f)}$R) in combination with GRK2.

The 5-HT/GRK2-mediated attenuation of 5-HT$_4$R splice variant-stimulated cAMP formation was examined. Despite a significant difference in the number of potential phosphate acceptor sites after the splice site (Leu[358]) (four in 5-HT$_{4(a)}$R, six in 5-HT$_{4(b)}$R, one in 5-HT$_{4(c)}$R, and none in variant 5-HT$_{4(f)}$R) (Fig. 3*A*), a similar uncoupling was observed (Fig. 3*B*). The absence of a role for these residues in 5-HT$_4$R uncoupling was confirmed by the fact that a receptor mutant (Δ358) truncated at the level of the Leu[358] splice site was similarly uncoupled (Fig. 4*C*).

Ser/Thr clusters (three or four consecutive Ser/Thr residues) have been reported previously to be better potential phosphate acceptor sites for GRK than scattered Ser/Thr residues (33). In
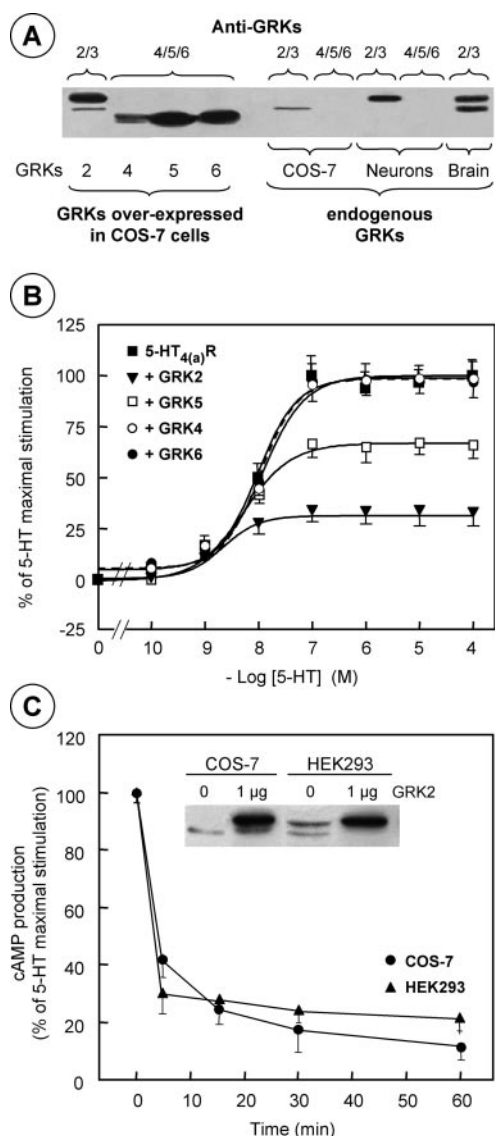
Molecular Events in the Uncoupling and Endocytosis of 5-HT$_4$Rs

FIG. 2. **Effect of overexpression of GRKs on 5-HT$_4$R uncoupling.** *A*, GRKs from COS-7 cells and colliculus neurons were subjected to Western blot analysis. COS-7 cells were transiently transfected with 1 μg of each GRK cDNA (GRK2/4/5/6). The day after transfection, the levels of GRK overexpression in COS-7 cells were compared with the levels of endogenous GRKs expressed in COS-7 cells and colliculus neurons by Western blotting of equal amounts of whole cell lysates. The monoclonal antibodies used to develop immunoreactive bands do not differentiate between GRK2 and GRK3 or between GRK4/5 and GRK6. The Western blot shown is representative of three independent experiments. *B*, 5-HT$_{4(a)}$R-mediated cAMP formation was differentially affected by GRKs. COS-7 cells were transiently transfected with 5-HT$_{4(a)}$R (100 ng of cDNA) alone or in combination with GRK2, GRK4, GRK5, or GRK6 (1 μg of each GRK cDNA). The day after transfection, cells were stimulated for 5 min at 37 °C with increasing concentrations of 5-HT in the presence of a phosphodiesterase inhibitor (Ro 20-1724). Data are expressed as a percentage of the maximum cAMP response produced in cells in which the receptor was expressed alone. Basal and 5-HT-stimulated cAMP values in this latter situation were 32 ± 4 and 172 ± 6 pmol/well, respectively. Results are the mean of three independent experiments. *C*, overexpression of GRK2 in COS-7 and HEK293 cells reproduced the time course of 5-HT-induced uncoupling found in colliculus neurons. COS-7 and HEK293 cells expressing 5-HT$_{4(a)}$R (100 ng of cDNA) were cotransfected or not with GRK2 (1 μg of cDNA). The expression levels of endogenous GRK2 in COS-7 or HEK293 cells were revealed by Western blotting with anti-GRK2 antibody and compared with the expression levels in transfected cells. Twenty-four hours after transfection, cells were pretreated with 10 μM 5-HT for the indicated uncoupling periods (0–60 min). Cells were extensively washed and incubated with 30 μM 5-HT for a 5-min cAMP accumulation period in the presence of Ro 20-1724 (0.1 mM) at 37 °C. Data are expressed as a percentage of the 5-HT stimulation obtained in

5-HT$_4$Rs, a cluster of Ser and Thr residues is localized upstream of the splice site (Leu[358]) and is common to all variants (Fig. 3*A*). To determine whether this cluster is involved in 5-HT/GRK2-mediated uncoupling, we examined the uncoupling of the truncated Δ346 mutant, which lacks the cluster of Ser/Thr residues common to all variants. 5-HT/GRK2-mediated uncoupling was independent of the presence or absence of the Ser/Thr clusters (Fig. 4*C*). This was confirmed by using the Δ358Ala mutant, in which each of the Ser and Thr residues of the cluster were replaced with alanine residues (Fig. 4*C*). Taken together, these results suggest that the Ser and Thr residues in the C-terminal domain are not necessary for 5-HT$_4$R uncoupling. Note that HA-tagged WT 5-HT$_{4(a)}$R and all of the truncated mutants (HA-Δ358, HA-Δ358Ala, and HA-Δ346) were expressed at the cell surface at comparable levels (Fig. 4*B*).

GRK2 Kinase Activity Is Not Necessary for 5-HT$_4$R Uncoupling—The absence of any role for the C-terminal Ser/Thr residues in 5-HT/GRK2-mediated uncoupling does not exclude the potential involvement of other Ser or Thr residues present in the intracellular loops. Because several reports (22, 23, 25) have shown that the kinase activity of GRK is not always necessary to obtain GRK-mediated uncoupling, we assessed the effect of the kinase-dead GRK2(K220R) mutant, in which the kinase activity was disrupted by site-directed mutagenesis. GRK2(K220R) was as efficient as and only slightly less potent than native GRK2 in 5-HT$_4$R uncoupling (Fig. 5, *A* and *B*). The fact that GRK2 uses a phosphorylation-independent mechanism to trigger 5-HT$_4$R uncoupling was confirmed by the presence of a marked increase in 5-HT-dependent phosphorylation of 5-HT$_4$R when expressed with GRK2 and, in contrast, the absence of receptor phosphorylation when expressed alone or in the presence of the kinase-dead GRK2(K220R) mutant (Fig. 5*C*).

5-HT$_4$R Uncoupling and Endocytosis Require Different GRK2 Expression Levels—To determine whether the level of GRK2 is important for 5-HT$_4$R endocytosis in transiently transfected cells, we examined the agonist-induced loss of surface HA-tagged 5-HT$_4$R in HEK293 cells in the presence and absence of GRK2 overexpression. The amount of HA-tagged 5-HT$_4$R remaining on the cell surface was quantified by ELISA (Fig. 6*A*) and used as a measure of receptor internalization. In HEK293 cells, agonist induced a 36% loss of surface receptor after a 30-min exposure. To our surprise, overexpression of GRK2 did not potentiate the decrease in surface 5-HT$_4$R (Fig. 6*A*). These observations suggest that endogenous levels of GRK2 are insufficient for rapid uncoupling, but are sufficient for agonist-induced receptor internalization.

To analyze the nature of the endocytosis, we followed the ability of c-Myc-tagged 5-HT$_{4(a)}$R constructs to associate with β-arrestin-2-YFP and to undergo endocytosis. We used a β-arrestin-2-YFP translocation assay and fluorescence microscopy in HEK293 cells. Cell-surface receptors were prelabeled with primary antibodies prior to agonist stimulation. In the absence of agonist, β-arrestin-2 was distributed throughout the cytoplasm in cells expressing the receptor, whereas c-Myc-tagged 5-HT$_{4(a)}$R was observed at the plasma membrane. Following a 15-min stimulation with 5-HT, an extensive co-localization of both β-arrestin-2-YFP and the c-Myc-tagged receptor appeared as punctuate fluorescence labeling of endocytic vesicles (Fig. 6*B*). After a 45-min period of agonist exposure, a change in the

the absence of transfected GRK2. Basal and 5-HT-stimulated cAMP values were 30 ± 4 and 150 ± 3 pmol/well, respectively, when 5-HT$_{4(a)}$R was transfected alone in COS-7 cells and 5 ± 2 and 29 ± 5 pmol/well, respectively, when 5-HT$_{4(a)}$R was transfected alone in HEK293 cells. Results represent the means ± S.E. of three independent experiments performed in triplicate.
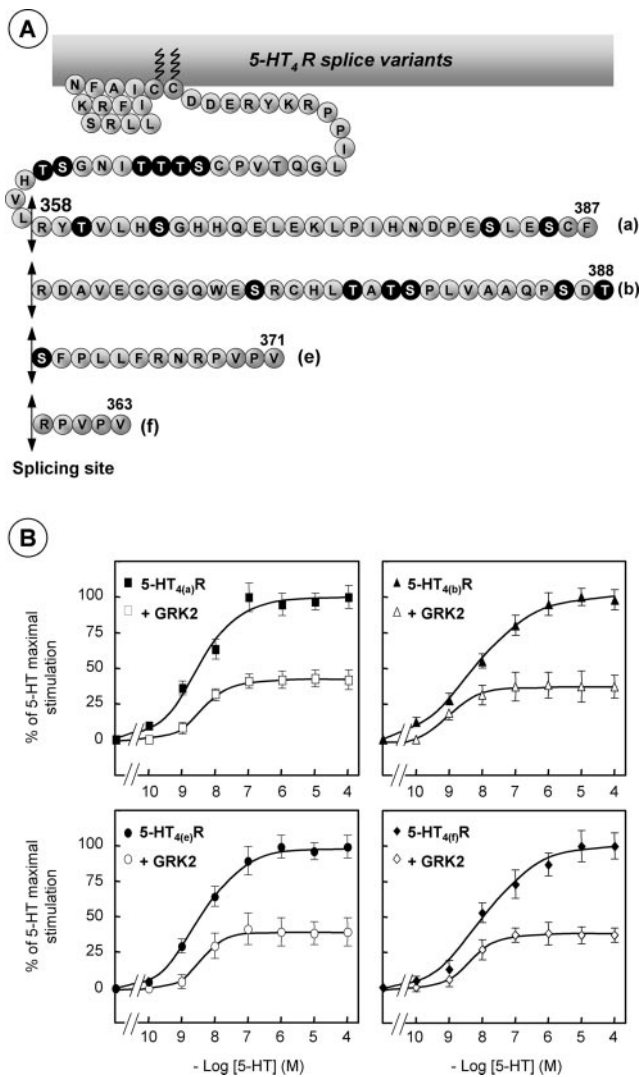
FIG. 3. **GRK2 mediates similar attenuation of receptor-stimulated cAMP formation for the four 5-HT$_4$R splice variants, despite different Ser/Thr compositions within the specific C-terminal sequence.** *A*, amino acid compositions of the C-terminal tails of the 5-HT$_4$R variants. The four 5-HT$_4$R variants have identical sequence up to Leu[358], after which both the length and composition of their C-terminal domains differ. Serine/threonine residues are represented by *black circles*. *B*, GRK2 mediates similar attenuation of 5-HT$_4$R variant-stimulated cAMP formation. 5-HT$_4$R-mediated cAMP formation was measured in COS-7 cells transfected with each 5-HT$_4$R splice variant (100 ng of plasmid) in the presence or absence of overexpressed GRK2. The day following transfection, cells were stimulated for 5 min with increasing concentrations of 5-HT in the presence of Ro 20-1724. Data are expressed as a percentage of the maximum cAMP response produced by the receptor without overexpression of GRK2. Basal and 5-HT-stimulated cAMP values when the 5-HT$_4$R splice variant was expressed alone were 36 ± 4 and 185 ± 8 pmol/well, respectively, for 5-HT$_{4(a)}$R; 31 ± 4 and 160 ± 5 pmol/well, respectively, for 5-HT$_{4(b)}$R; 38 ± 6 and 190 ± 8 pmol/well, respectively, for 5-HT$_{4(e)}$R; and 26 ± 4 and 154 ± 8 pmol/well, respectively, for 5-HT$_{4(f)}$R. Results are the means ± S.E. of three independent experiments. COS-7 cells were transfected with 100 ng of each HA-tagged 5-HT$_4$R splice variant cDNA with or without 1 μg of pcDNA3.1-GRK2. Receptor expression levels were similar for all of the variants (between 960 and 1100 fmol/mg of protein). When expressed with GRK2, the expression levels were between 1000 and 1150 fmol/mg of protein. Relative cell-surface expression of HA-tagged 5-HT$_4$R was determined by ELISA. The mean of chemiluminescence values indicated that, before any treatment, all variants were similarly expressed at the cell surface in either the presence or absence of GRK2.

pattern of staining was observed, *i.e.* the c-Myc-5-HT$_{4(a)}$R·β-arrestin-2-YFP complexes translocated to a perinuclear compartment (Fig. 6*B*).
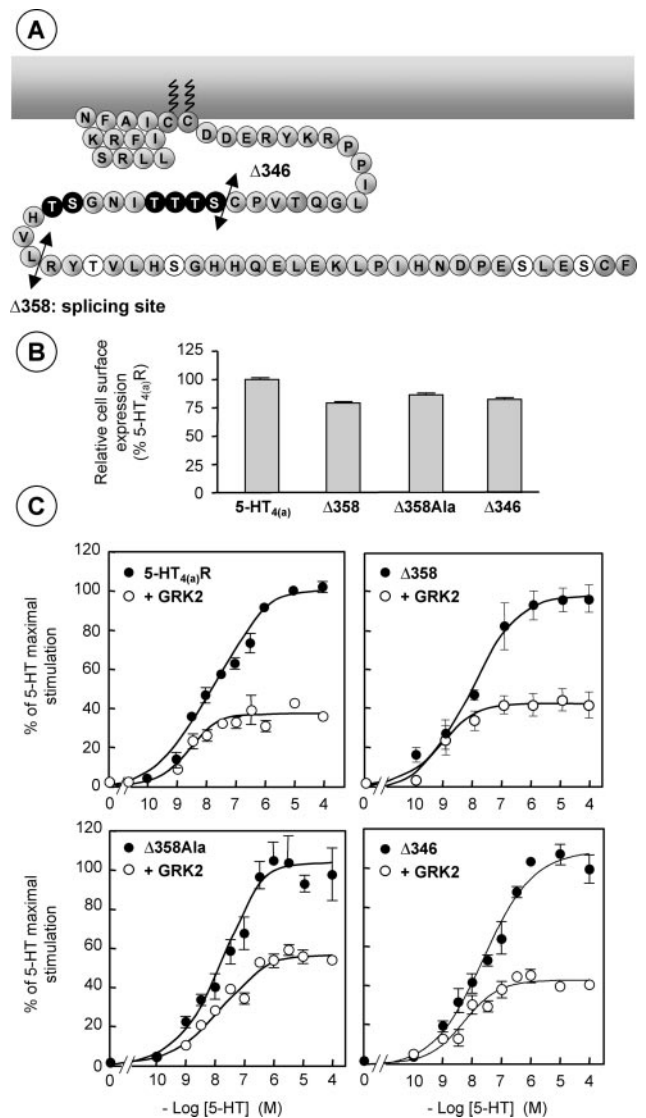

FIG. 4. **GRK2 mediates the uncoupling of 5-HT$_4$R, even in the absence of the Ser/Thr cluster upstream of the Leu[358] splice site within the C-terminal domain.** *A*, topology of the C-terminal amino acid sequences of 5-HT$_{4(a)}$R and a series of truncated mutants. Putative Ser/Thr phosphate acceptor sites are represented by *black circles*. The *arrows* indicates the point of truncation on the C-terminal tail. *B*, relative cell-surface expression of WT 5-HT$_{4(a)}$R and its mutants. COS-7 cells were transfected with 100 ng of HA-5-HT$_{4(a)}$R, HA-Δ358, Δ358Ala, or HA-Δ346. The day after transfection, ELISA was performed to quantify relative cell-surface receptor expression before agonist stimulation. Results are expressed as a percentage of HA-tagged 5-HT$_{4(a)}$R. Data represent the means ± S.E. of three independent experiments. *C*, effect of GRK2 overexpression on WT and mutant receptor-stimulated cAMP formation. 5-HT-induced cAMP production was measured in COS-7 cells transfected with 100 ng of HA-5-HT$_{4(a)}$R, HA-Δ358, HA-Δ358Ala, or HA-Δ346 in the presence or absence of overexpression of GRK2 (1 μg of GRK2 cDNA). Twenty-four hours after transfection, cells expressing the receptors in either the absence or presence of GRK2 overexpression were stimulated for 5 min with increasing concentrations of 5-HT in the presence of Ro 20-1724 (0.1 mM). Data are expressed as a percentage of the maximum cAMP response produced by each receptor without overexpression of GRK2. When 5-HT$_4$R was expressed alone, basal and 5-HT-stimulated cAMP values were 34 ± 4 and 182 ± 8 pmol/well, respectively, for the WT receptor; 36 ± 4 and 177 ± 8 pmol/well, respectively, for Δ358; 28 ± 4 and 162 ± 8 pmol/well, respectively, for Δ358Ala; and 40 ± 6 and 192 ± 7 pmol/well, respectively, for Δ346. Results are the means ± S.E. of three independent experiments.

Given the important roles that phosphorylated Ser and Thr play in promoting receptor/β-arrestin interaction (33), we examined whether some specific Ser/Thr residues in the 5-HT$_4$R
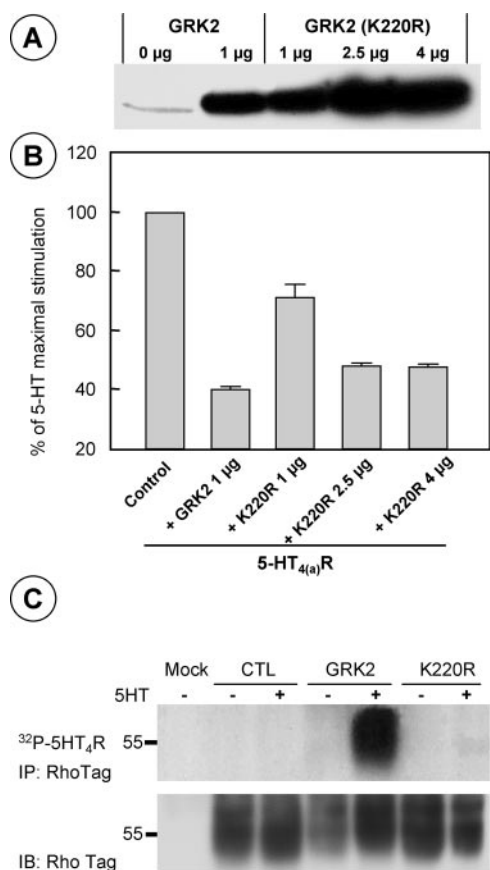
FIG. 5. **GRK2 kinase activity is not required for 5-HT₄R uncoupling.** COS-7 cells were transiently transfected with 5-HT$_{4(a)}$R (100 ng of plasmid) with either GRK2 (1 μg) or different amounts of dominant-negative GRK2(K220R) (1–4 μg). *A*, the expression levels of transfected GRK2 and GRK2(K220R) were revealed by Western blotting of whole cell lysates 24 h after transfection. *B*, the effect of overexpression of GRK2 and GRK2(K220R) was tested for cAMP production in response to 30 μM 5-HT for 5 min in the presence of Ro 20-1724. Data are expressed as a percentage of the maximum cAMP response produced by 5-HT$_{4(a)}$R expressed alone. Basal and 5-HT-stimulated cAMP values were 32 ± 4 and 177 ± 6 pmol/well, respectively. ELISA were performed to quantify cell-surface receptor expression before and after agonist stimulation. Data represent the means ± S.E. for three independent experiments. *C*, the phosphorylation state of 5-HT$_{4(a)}$R was studied following metabolic labeling with ^{32}P in the absence or presence of GRK2 or GRK2(K220R) overexpression. Cells transfected with 5-HT$_{4(a)}$R (1 μg of plasmid) alone or with either GRK2 (1 μg) or GRK2(K220R) (2.5 μg) were incubated (+) or not (−) with 10 μM 5-HT for 10 min. The receptor was purified by immunoprecipitation (*IP*) using anti-Rho tag monoclonal antibody. The identity of the bands was confirmed by Western blot analysis (immunoblotting (*IB*)) using mouse anti-Rho tag antibody. The autoradiograms shown are representative of three independent experiments. *CTL*, control.

C-terminal domain are involved in 5-HT₄R/β-arrestin-2 association and endocytosis. We began by analyzing and comparing the endocytosis of the 5-HT$_{4(a)}$R, 5-HT$_{4(b)}$R, and 5-HT$_{4(e)}$R splice variants as well as the endocytosis of the Δ358 mutant, which shares the sequence common to all of the variants. As shown in Fig. 6*B*, all of the variants, as well as the Δ358 mutant, exhibited similar endocytosis kinetics and the ability to associate with β-arrestin-2. Consequently, Ser/Thr residues scattered over specific C-terminal domains of the 5-HT$_{4(a)}$R, 5-HT$_{4(b)}$R, and 5-HT$_{4(e)}$R splice variants (Fig. 3*A*) did not seem to be implicated in the 5-HT₄R association with β-arrestin-2 and endocytosis (Fig. 6*B*). When cells were incubated for 15 min in the presence of agonist, washed extensively, and subjected to an additional incubation in the absence of agonist for 6 h, all of the 5-HT₄R splice variants that formed stable complexes with β-arrestin translocated to endosomes in a perinu-
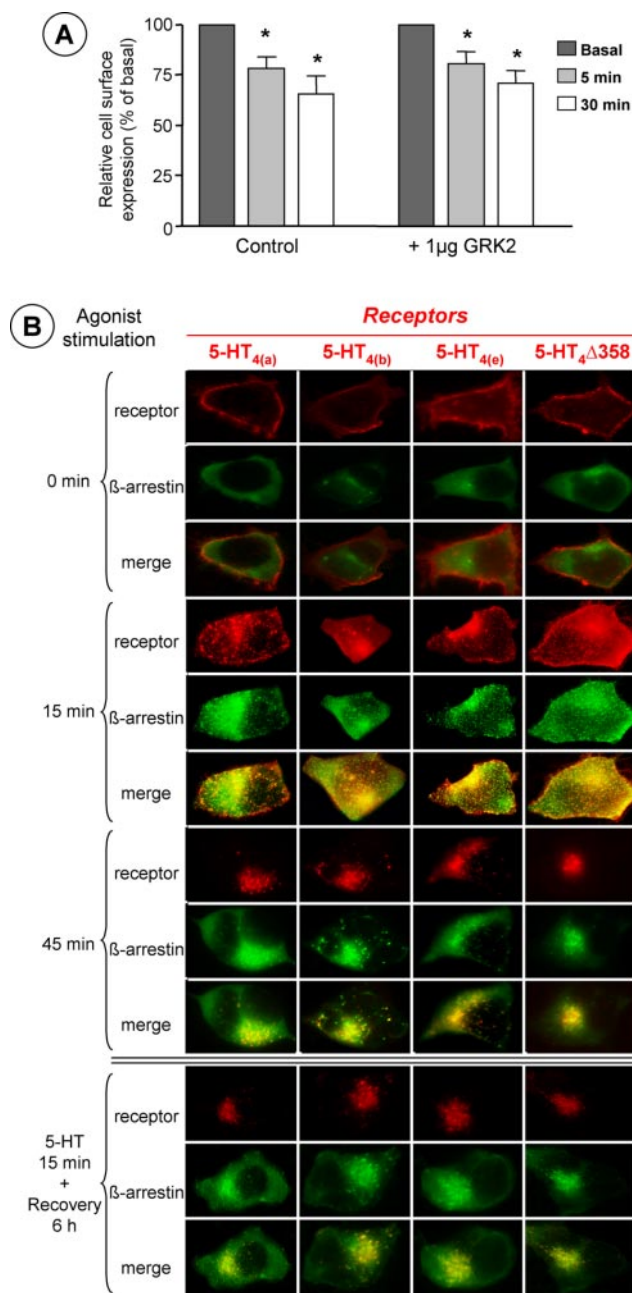

FIG. 6. **Overexpression of GRK2 is not required for 5-HT₄R endocytosis in HEK293 cells.** Similar 5-HT₄R/β-arrestin endocytosis was observed, regardless of the 5-HT₄R splice variant considered. *A*, cell-surface expression of HA-tagged 5-HT₄R (100 ng of plasmid) transfected alone in HEK293 cells or in combination with 1 μg of cDNA encoding GRK2 was determined by ELISA before and after stimulation with 5-HT (10 μM) for 5 and 30 min as described under "Experimental Procedures." Data represent the means ± S.E. of four independent experiments. *, $p <$ 0.01 (significantly different from the corresponding cells before 5-HT treatment). *B*, HEK293 cells were transiently cotransfected with 600 ng of c-Myc-tagged 5-HT$_{4(a)}$R, 5-HT$_{4(b)}$R, or 5-HT$_{4(e)}$R splice variant or Δ358 mutant in combination with 1 μg of GRK2 and 0.3 μg of β-arrestin-2-YFP. Intact cells were immunostained with anti-c-Myc antibody before activation of 5-HT₄R. The *upper panels* show the distribution of β-arrestin-2-YFP and c-Myc-tagged 5-HT₄R splice variants either before (0 min; control) or after (15 and 45 min) addition of 5-HT (30 μM) to the culture medium. The *lower panels* show cells that were stimulated for 15 min with agonist and then extensively washed and subjected to an additional incubation in agonist-free medium for 6 h. Cells were fixed either after a stimulation period in the presence of the agonist or after a period of recovery in agonist-free medium. Immunoreactivity was revealed with Alexa Fluor 594-conjugated secondary antibodies. Fluorescence microscopy was then used to visualize the redistribution of antibody-labeled receptors and β-arrestin-2-YFP. Note that the majority of vesicles containing internalized 5-HT₄R also contained β-arrestin-2-YFP.
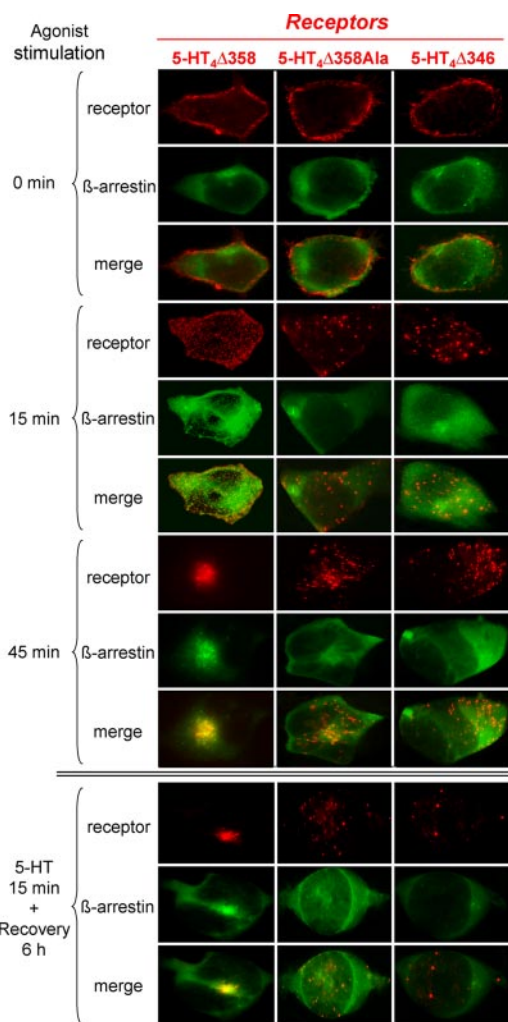
FIG. 7. **β-Arrestin-2 is not recruited by the truncated 5-HT$_4$R mutants lacking the Ser/Thr cluster within the C-terminal domain.** HEK293 cells were transiently cotransfected with 600 ng of c-Myc-Δ358, c-Myc-Δ358Ala, or c-Myc-Δ346 in combination with 1 μg of GRK2 and 0.3 μg of β-arrestin-2-YFP. Intact cells were immunostained with anti-c-Myc antibody before activation of 5-HT$_4$R. The *upper panels* show the distribution of β-arrestin-2-YFP and c-Myc-tagged 5-HT$_4$R either before (0 min; control) or after (15 and 45 min) addition of 30 μM 5-HT to the culture medium at 37 °C. The *lower panels* show cells that were stimulated with agonist for 15 min and then extensively washed and subjected to an additional incubation in agonist-free medium for 6 h. Cells were fixed after treatments. Immunoreactivity was revealed with Alexa Fluor 594-conjugated secondary antibodies. Fluorescence microscopy was then used to visualize the redistribution of the antibody-labeled receptor and β-arrestin-2-YFP. Note the prominent colocalization of activated c-Myc-Δ358 with β-arrestin-2-YFP, whereas mutants lacking the Ser/Thr cluster upstream of the Leu[358] splice site (Δ358Ala and Δ346) did not co-localize with β-arrestin-2-YFP.

clear region, where the complexes were preserved for >6 h, as shown in Fig. 6B (*lower panels*).

β-Arrestin-dependent Endocytosis of 5-HT$_4$R Is Dependent on the Ser/Thr Clusters within the Receptor C-terminal Domain—We analyzed the endocytosis of the c-Myc-Δ346 and c-Myc-Δ358Ala mutants to investigate whether the common Ser/Thr cluster upstream of the Leu[358] splice site is implicated in c-Myc-5-HT$_4$R/β-arrestin-2-YFP association. Both mutants failed to co-localize with β-arrestin-2 in endocytic vesicles (Fig. 7). However, these mutants still endocytosed, but in a β-arrestin-independent manner. Furthermore, in contrast to WT 5-HT$_{4(a)}$R and the Δ358 mutant, Δ346 and Δ358Ala did not concentrate in the perinuclear compartment (Fig. 7). Thus, the common Ser/Thr cluster is an absolute requirement for β-arrestin-
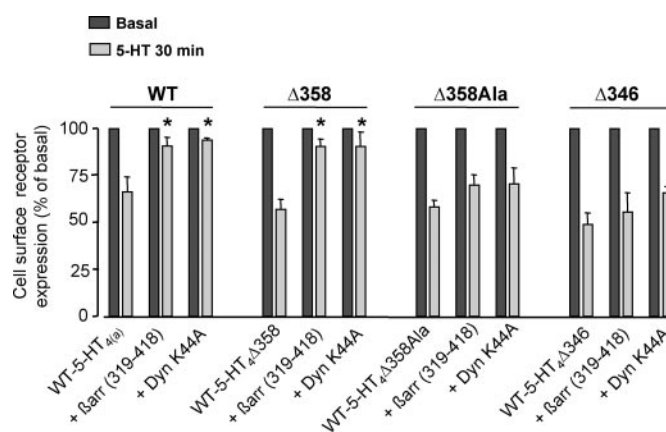

FIG. 8. **Dominant-negative β-arrestin-(319–418) and dominant-negative dynamin(K44A) inhibit agonist-induced internalization of both truncated 5-HT$_4$R and C-terminal mutants.** HEK293 cells were transiently transfected with GRK2 and the c-Myc-tagged WT receptor, Δ358, Δ358Ala, or Δ346 (100 ng of each plasmid) in combination with either dominant-negative β-arrestin-(319–418) (*βarr (319–418)*; 1 μg) or dominant-negative dynamin(K44A) (*Dyn K44A*; 1 μg). Cells were pretreated (*dark gray bars*) or not (*light gray bars*) for 30 min at 37 °C. Cells were then fixed, and the amount of receptor remaining on the cell surface was quantified by ELISA. Results shown are the means ± S.E. of four separate experiments performed in triplicate. *, $p < 0.01$ (significantly different from the corresponding WT receptor and Δ358 mutant in the absence of the dominant-negative proteins).

dependent endocytosis as well as for normal trafficking. The importance of 5-HT$_4$R/β-arrestin association in receptor endocytosis was quantified by ELISA. As shown in Fig. 8, agonist induced a 36 ± 7% loss of surface receptor after a 30-min incubation. Similar endocytosis was obtained with the Δ358, Δ346, and Δ358Ala mutants. However, whereas the endocytosis of the wild-type receptor and Δ358 mutant was blocked by dominant-negative β-arrestin-(319–418) and dominant-negative dynamin(K44A), the endocytosis of the Δ346 and Δ358Ala mutants was unaffected by these dominant-negative proteins (Fig. 8).

To investigate whether the observed differences in receptor endocytosis would differentially affect the recycling of the receptors, cells expressing either the Δ346 or Δ358Ala mutant, both of which are unable to interact with β-arrestin, were incubated with agonist for 15 min and then subjected to an additional incubation in the absence of agonist for 6 h. As shown in Fig. 7 (*lower panels*), the Δ358Ala and Δ346 receptor mutants, which lack interaction with β-arrestin, were retained in small vesicles distributed in the cytosol and preserved for >6 h.

To determine whether 5-HT$_4$R follows the same endocytosis in native colliculus neurons, we analyzed the agonist-mediated internalization of 5-HT$_4$R in intact neuronal cells expressing Rho-tagged 5-HT$_4$R. The contribution of the β-arrestin/dynamin pathway to this endocytosis was examined by ELISA.

As shown in Fig. 9A, in the absence of any stimulation, 5-HT$_4$Rs were strictly expressed on the membrane. Indeed, no labeling was obvious in orthogonal sections of the neurons. In contrast, 5-HT induced a significant change in cell-surface expression. An unequivocal labeling of endocytosed receptors was noticeable in both the *Z* section and orthogonal sections of the neurons.

A more quantitative assessment of 5-HT$_4$R endocytosis was carried out by ELISA. A 30-min stimulation induced a loss of 34% of surface receptors (Fig. 9B). In addition, Fig. 9B clearly shows that 5-HT$_4$R endocytosis in colliculus neurons was largely reduced by dominant-negative β-arrestin-(319–418) and dominant-negative dynamin(K44A). As in HEK293 cells, WT 5-HT$_{4(a)}$R endocytosis in colliculus neurons was β-arrestin/dynamin-dependent.
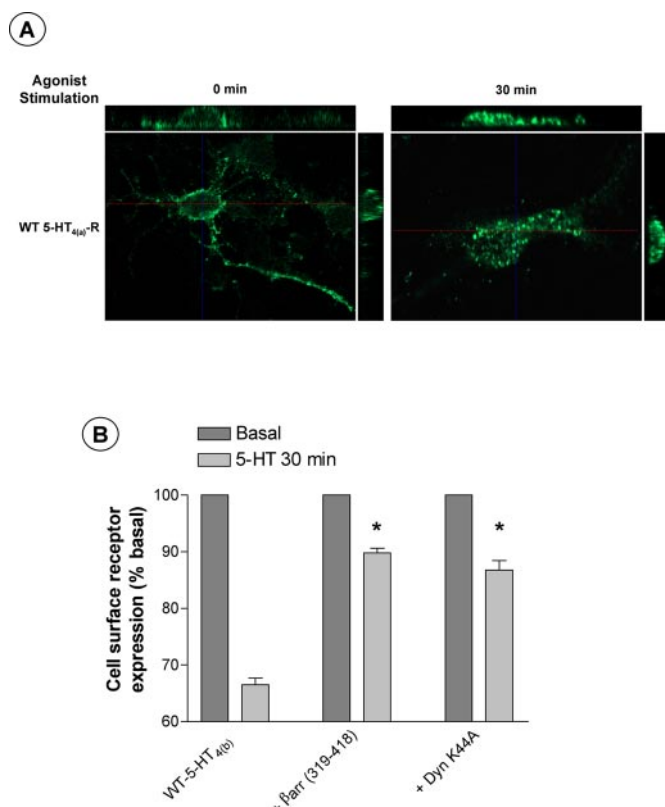
FIG. 9. **5-HT induces 5-HT$_4$R/β-arrestin- and dynamin-dependent endocytosis in colliculus neurons.** *A*, colliculus neurons were transiently transfected with 2.5 μg of Rho-tagged 5-HT$_{4(a)}$R using the mouse neuron Nucleofector™ kit. Intact cells were immunostained with anti-Rho antibody before activation of 5-HT$_4$R. The distribution of Rho-tagged 5-HT$_4$R is shown either before (0 min) or after (30 min) addition of 10 μM 5-HT to the culture medium at 37 °C. Immunoreactivity was revealed with Alexa Fluor 488-conjugated secondary antibodies. Confocal microscopy was then used to visualize the redistribution of antibody-labeled receptors. *B*, colliculus neurons were transiently transfected with Rho-tagged 5-HT$_4$R (2.5 μg) in combination with either dominant-negative β-arrestin-(319–418) (*βarr (319–418)*; 2 μg), or dominant-negative dynamin(K44A) (*Dyn K44A*; 2 μg). Neurons were pretreated (*light gray bars*) or not (*dark gray bars*) for 30 min at 37 °C with 10 μM 5-HT. Neurons were then fixed, and the amount of receptor remaining on the cell surface was quantified by ELISA. Results shown are the means ± S.E. of two separate experiments performed in sextuplicate. *, $p < 0.01$ (significantly different from the corresponding 5-HT$_4$Rs in the absence of the dominant-negative proteins).

Three main conclusions can be drawn from these experiments. First, the common cluster of Ser and Thr residues upstream of the Leu[358] splice site is an absolute requirement for normal β-arrestin/dynamin-dependent endocytosis and trafficking. This indicates that the endocytosis of 5-HT$_4$R, as opposed to its uncoupling, requires the kinase activity of GRK2 and the phosphorylation of Ser/Thr clusters common to all splice variants within the C-terminal domain to traffic with β-arrestin. Second, in the absence of Ser/Thr clusters, the receptor is still endocytosed, but in a β-arrestin/dynamin-independent manner. Third, β-arrestin is not the only trafficking protein able to control receptor internalization of 5-HT$_4$R.

The Kinase-deficient GRK2 Mutant Suppresses β-Arrestin-dependent Endocytosis and Promotes β-Arrestin-independent Endocytosis—We next determined whether the overexpression of GRK2(K220R) in HEK293 cells could block or induce endocytosis of the WT receptor. After a 30-min stimulation with 5-HT, the endocytosis of 5-HT$_{4(a)}$Rs was greater when GRK2(K220R) was expressed (Fig. 10*A*) instead of the native GRK2 kinase (Fig. 6*A*). Note that, in the presence of GRK2(K220R), dominant-negative β-arrestin-(319–418) was
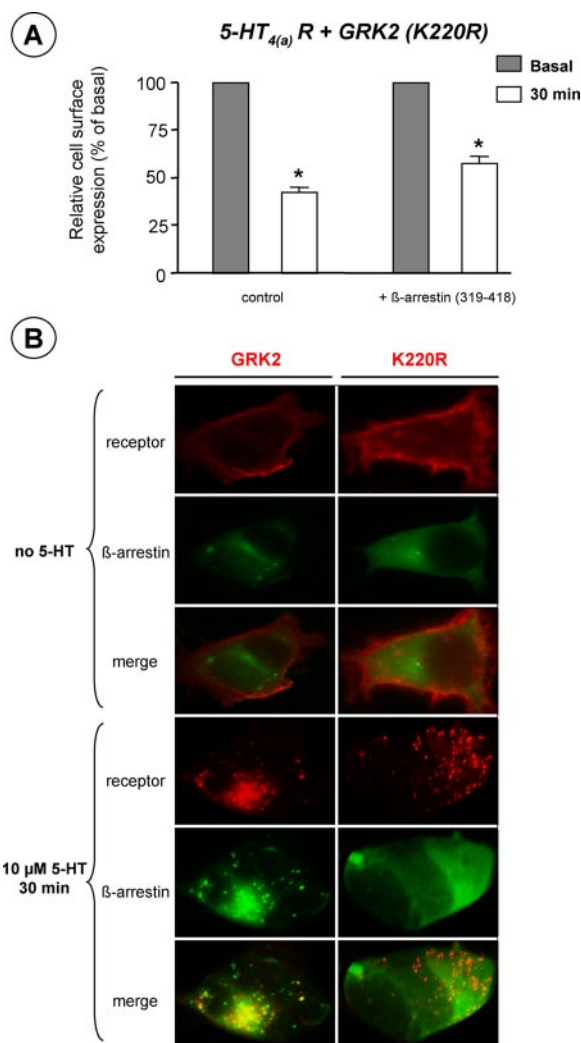
FIG. 10. **The kinase-deficient GRK2(K220R) mutant induces 5-HT$_4$R/β-arrestin-2-independent endocytosis.** *A*, the relative cell-surface expression of HA-tagged 5-HT$_4$R (100 ng) transfected in HEK293 cells in combination with 2.5 μg of GRK2(K220R) was determined before and after stimulation with 5-HT (30 μM) for 5 and 30 min by ELISA and in the absence and presence of dominant-negative β-arrestin-(319–418) as described under "Experimental Procedures." Data represent the means ± S.E. of four independent experiment. *, $p < 0.01$ (significantly different from the corresponding cells before 5-HT treatment). *B*, HEK293 cells transiently expressing c-Myc-tagged 5-HT$_4$R in combination with β-arrestin-2-YFP and 1 μg of GRK2 (*left panels*) or 2.5 μg of GRK2(K220R) (*right panels*) were incubated in the absence (control) or presence of 30 μM 5-HT for 15 or 45 min at 37 °C or for 15 min with agonist and then extensively washed and subjected to an additional incubation in agonist-free medium for 6 h. Cells were fixed and processed for immunofluorescence microscopy. These images are representative of many cells examined in at least three independent experiments. Fluorescence microscopy was then used to visualize the redistribution of antibody-labeled receptors, and β-arrestin-2-YFP was visualized. Note the prominent co-localization of activated c-Myc-tagged 5-HT$_4$R with β-arrestin-2-YFP when GRK2 was coexpressed and the total absence of co-localization when the kinase-deficient GRK2(K220R) mutant was coexpressed.

almost inactive in reducing endocytosis (Fig. 10*A*). This is also directly visualized in Fig. 10*B*. In the presence of GRK2(K220R), β-arrestin-dependent endocytosis of 5-HT$_4$R was not observed. In contrast, the endocytosis of 5-HT$_4$Rs was clearly present and distributed in vesicles in which β-arrestin was absent (Fig. 10*B*, *right panels*). These results support the conclusion that kinase activity and Ser/Thr clusters are required for normal β-arrestin/dynamin-dependent endocytosis and trafficking of 5-HT$_4$R.

DISCUSSION

It is important to study the molecular mechanisms of signal transduction in native tissues because they can be substantially different from those in heterologous cell lines, as shown recently (37, 45, 46). This is particularly important for studying desensitization of GPCRs, which are extremely dependent on the specific molecular and cellular characteristics of the receptor as well as the cell in which they are expressed. This has been recently reported for γ-aminobutyric acid type B receptors (25), which were desensitized in cerebellar granule cell neurons, but not in HEK293 cells. The reason is that GRK4, which is required for γ-aminobutyric acid type B receptor desensitization, is absent in HEK293 cells. Similarly, we have shown here that the rapid and marked uncoupling of 5-HT₄R observed in colliculus neurons was not observed when the receptor was expressed in COS-7 or HEK293 cells. One of the main reasons is probably the absence of significant expression of GRK2 in COS-7 cells and only modest expression in HEK293 cells (30, 47). In contrast, colliculus neurons expressed a high concentration of GRK2, and no other GRK was significantly expressed in these neurons. The main role for GRK2 in 5-HT₄R uncoupling was confirmed by the fact that overexpression of GRK2 in COS-7 and HEK293 cells mimicked the 5-HT₄R uncoupling characteristics observed in neurons. However, GRK5 was less active, and both GRK4 and GRK6 were inactive. The GRK2-mediated uncoupling of 5-HT₄Rs was also phosphorylation-independent. Indeed, no difference in GRK2-mediated uncoupling was observed between the different 5-HT₄R splice variants, which differ in the number of Ser and Thr residues present in their specific C-terminal domains. Uncoupling remained unaffected when the cluster of Ser and Thr residues localized upstream of the Leu³⁵⁸ splice site was removed by truncation or mutated to Ala. Finally, full uncoupling was observed when the kinase-deficient GRK2 mutant was expressed. There are several reports showing phosphorylation-independent reduction of GPCR agonist response by kinase-deficient GRK2 or GRK4 (21, 23, 25). However, only a few studies have reported the role of kinase-deficient GRK in the classical agonist-promoted desensitization paradigm (24, 25, 48). Interestingly, two recent studies, one concerning γ-aminobutyric acid type B receptors and GRK4 (25) and the other concerning M1 muscarinic receptors and GRK2 (46), demonstrated a kinase-independent role of GRKs in neurons. To date, the mechanism by which GRK2 induces 5-HT₄R uncoupling in a phosphorylation-independent manner remains to be studied. We can only speculate based on the known properties of GRK2. This kinase has been proposed to interact with many signaling proteins capable of influencing signaling efficacy. These include Gα protein(s) (mainly Gα_q) via the N-terminal RGS (regulators of G protein signaling) domain of GRK2, G$\beta\gamma$ and phosphatidylinositol diphosphate via the C-terminal pleckstrin homology domain of GRK2, clathrin, GIT1 (a member of the GRK-interacting protein family), caveolin, phosphoinositide 3-kinase-α and -γ, and Ca²⁺ sensor protein (reviewed in Ref. 49). Many of these interactions, especially with G$\beta\gamma$, are probably involved in the kinase-independent uncoupling of 5-HT₄Rs by GRK2.

Following the early work of Lefkowitz and co-workers (31), Su *et al.* (29) were the first to demonstrate that functional uncoupling precedes receptor migration to a buoyant fraction (likely endocytic vesicles). Since these early days, much data have indicated that uncoupling and endocytosis are distinct steps (50–52). However, dissociating the two events kinetically or in terms of molecular events is not always easy. Here, we have shown that the uncoupling and endocytosis of 5-HT₄Rs require very different GRK2 expression levels and distinct

molecular events. Indeed, although the modest endogenous expression level of GRK2 in HEK293 cells was sufficient to obtain endocytosis of 5-HT₄Rs that was both β-arrestin- and dynamin-dependent, it was totally insufficient to achieve the marked 5-HT₄R uncoupling observed in neurons. There is also another clear difference; uncoupling was independent of phosphorylation, whereas 5-HT₄R/β-arrestin-dependent endocytosis required the C-terminal Ser/Thr cluster as well as the kinase activity of GRK2. Indeed, we clearly showed that the kinase-deficient GRK2 mutant inhibited 5-HT₄R/β-arrestin-dependent endocytosis, but promoted 5-HT₄R/β-arrestin-independent endocytosis. Thus, phosphorylation of the 5-HT₄R C-terminal domain seems to be absolutely necessary for β-arrestin recruitment. This model contrasts with those of the dopamine D_1 receptor, in which phosphorylation of Ser/Thr permits access of arrestin to its receptor-binding domain rather than creating an arrestin-binding site *per se* (28). However, in our study, the Δ346 mutant, whose i₃ loop is easily accessible, did not associate with β-arrestin, whereas the Δ358 mutant, which possesses the Ser/Thr cluster, was always able to interact with β-arrestin. These results confirm that the Ser/Thr cluster in the 5-HT₄R C-terminal domain is necessary for β-arrestin association. However, our results do not demonstrate that the Ser/Thr cluster is "the binding site" for β-arrestin. This phosphorylated Ser/Thr cluster could be necessary for the proper conformation of the receptor to allow appropriate β-arrestin binding.

Following overexpression of the kinase-deficient GRK2 mutant, the receptor could be endocytosed, but in a β-arrestin/dynamin-independent manner. Several GPCRs are known to require β-arrestins for endocytosis. These include the metabotropic glutamate type 1d receptor (23), the secretin receptor (53), 5-HT₂ₐR (54), protease-activated receptor-1 (55), the prostacyclin receptor (56), the formyl peptide receptor (57), the m2 muscarinic receptor (58), leukotriene B₄ receptor-1 (30), and the neuropeptide Y1 receptor (59). GRK2 associated with the 5-HT₄Rs may directly interact with clathrin via a clathrin box (60), which is present in the C-terminal region of GRK2. Further work is needed to investigate this possible mechanism.

Whatever the theoretical interest of the β-arrestin-independent endocytosis, it is important to note that it is the β-arrestin/dynamin-dependent endocytosis that is of physiological significance. Indeed, β-arrestin-independent endocytosis was almost unobserved with WT 5-HT₄R in HEK293 cells. Moreover, 70% of 5-HT₄R endocytosis in colliculus neurons was blocked either by dominant-negative β-arrestin or by dominant-negative dynamin. Thus, β-arrestin and dynamin control 5-HT₄R endocytosis in neurons.

In this study, we further confirmed that the uncoupling and endocytosis processes are independent. Indeed, there is no correlation between the level of endocytosed 5-HT₄Rs and the level of uncoupling. In the absence of overexpressed GRK2, 36 $\pm$ 6% of the receptors were endocytosed (Fig. 6*A*), with very low (10 $\pm$ 5%) uncoupling (Fig. 1*D*). In the presence of overexpressed GRK2, the level of endocytosed receptors was similar, whereas the uncoupling was above 80% (Fig. 2*C*).

Once endocytosed, the 5-HT₄Rs showed no sign of recycling. Indeed, a 15-min stimulation of the receptor was sufficient to induce receptor trafficking to a perinuclear compartment, where the receptor bound by arrestin was retained for >6 h. This behavior clearly classifies the 5-HT₄Rs into class B GPCRs (33). We have recently reported that 5-HT₄Rs are associated with a series of GPCR-interacting proteins, including SNX-27 (sorting nexin-27) and the Na⁺/H⁺ exchanger regulatory factor (61). Although the role of GPCR-interacting proteins in 5-HT₄R endocytosis and recycling remains to be analyzed,

they have been shown to be clearly implicated in other GPCR systems (62, 63).

Several important physiological effects have been attributed to 5-HT$_4$Rs. A recent study provides evidence that stress-induced hypophagia and novelty-induced exploratory activity are attenuated in 5-HT$_4$R knockout mice (4). Moreover, Lucas *et al.* (64) reported the existence of a key function for 5-HT$_4$R in the complex network linking the medial prefrontal cortex to the dorsal raphe neurons. They proposed that 5-HT$_4$Rs exert a tonic and positive influence on a subpopulation of f5-HT neurons.

In the enteric nervous system, 5-HT$_4$Rs, which are presynaptic, have been shown to enhance transmitter levels and thus to strengthen neurotransmission in prokinetic pathways (6). 5-HT$_4$Rs also regulate respiratory neurons (5).

All of these recent findings favor an intriguing role for 5-HT$_4$R in the fine-tuning of neuronal activity. Therefore, it is important to understand how 5-HT$_4$R responsiveness can be regulated to design efficacious drugs controlling these functions. In view of the present data, it is perhaps not surprising that only partial agonists have been selected as therapeutic drugs acting on 5-HT$_4$Rs. Metoclopramide, cisapride, and tegaserod are used to treat gastrointestinal diseases, and SL650155 is the only 5-HT$_4$R ligand in development for brain disorders (65). Obviously, a complete study of the action of agonists (full and partial), antagonists, and inverse agonists on 5-HT$_4$R uncoupling and endocytosis has to be done.

REFERENCES

1. Bockaert, J., Fagni, L., and Dumuis, A. (1997) in *Handbook of Experimental Pharmacology: Serotoninergic Neurons and 5-HT Receptors in the CNS* (Baumgarten, H. G., and Göthert, M., eds) Vol. 129, pp. 439–465, Spinger-Verlag, Berlin
2. Bockaert, J., Claeysen, S., Compan, V., and Dumuis, A. (2004) *Curr. Drug Targets CNS Neurol. Disord.* **3,** 39–51
3. Marchetti-Gauthier, E., Roman, F. S., Dumuis, A., Bockaert, J., and Soumireu-Mourat, B. (1997) *Neuropharmacology* **36,** 697–706
4. Compan, V., Zhou, M., Grailhe, R., Gazzara, R. A., Martin, R., Gingrich, J., Dumuis, A., Brunner, D., Bockaert, J., and Hen, R. (2004) *J. Neurosci.* **24,** 412–419
5. Manzke, T., Guenther, U., Ponimaskin, E. G., Haller, M., Dutschmann, M., Schwarzacher, S., and Richter, D. W. (2003) *Science* **301,** 226–229
6. Gershon, M. D. (2004) *Aliment. Pharmacol. Ther.* **20,** Suppl. 7, 3–14
7. Bender, E., Pindon, A., van Oers, I., Zhang, Y. B., Gommeren, W., Verhasselt, P., Jurzak, M., Leysen, J., and Luyten, W. (2000) *J. Neurochem.* **74,** 478–489
8. Hiroi, T., Hayashi-Kobayashi, N., Nagumo, S., Ino, M., Okawa, Y., Aoba, A., and Matsui, H. (2001) *Biochem. Biophys. Res. Commun.* **289,** 337–344
9. Fagni, L., Dumuis, A., Sebben, M., and Bockaert, J. (1992) *Br. J. Pharmacol.* **105,** 973–979
10. Claeysen, S., Sebben, M., Becamel, C., Bockaert, J., and Dumuis, A. (1999) *Mol. Pharmacol.* **55,** 910–920
11. Ponimaskin, E. G., Profirovic, J., Vaiskunaite, R., Richter, D. W., and Voyno-Yasenetskaya, T. A. (2002) *J. Biol. Chem.* **277,** 20812–20819
12. Ansanay, H., Sebben, M., Bockaert, J., and Dumuis, A. (1992) *Mol. Pharmacol.* **42,** 808–816
13. Ponimaskin, E., Dumuis, A., Gaven, F., Barthet, G., Heine, M., Glebov, K., Richter, D. W., and Oppermann, M. (2005) *Mol. Pharmacol.*, **67,** 1434–1443
14. Ferguson, S. S., Zhang, J., Barak, L. S., and Caron, M. G. (1998) *Life Sci.* **62,** 1561–1565
15. Carman, C. V., and Benovic, J. L. (1998) *Curr. Opin. Neurobiol.* **8,** 335–344
16. Ferguson, S. S., and Caron, M. G. (1998) *Semin. Cell Dev. Biol.* **9,** 119–127
17. Ferguson, S. S. (2001) *Pharmacol. Rev.* **53,** 1–24
18. Bunemann, M., Frank, M., and Lohse, M. J. (2003) *Proc. Natl. Acad. Sci. U. S. A.* **100,** 16077–16082
19. Gainetdinov, R. R., Premont, R. T., Bohn, L. M., Lefkowitz, R. J., and Caron, M. G. (2004) *Annu. Rev. Neurosci.* **27,** 107–144
20. Luttrell, L. M., and Lefkowitz, R. J. (2002) *J. Cell Sci.* **115,** 455–465
21. Carman, C. V., Parent, J. L., Day, P. W., Pronin, A. N., Sternweis, P. M., Wedegaertner, P. B., Gilman, A. G., Benovic, J. L., and Kozasa, T. (1999) *J. Biol. Chem.* 274, 34483–34492
22. Freedman, N. J., Ament, A. S., Oppermann, M., Stoffel, R. H., Exum, S. T., and Lefkowitz, R. J. (1997) *J. Biol. Chem.* **272,** 17734–17743
23. Dhami, G. K., Anborgh, P. H., Dale, L. B., Sterne-Marr, R., and Ferguson, S. S. (2002) *J. Biol. Chem.* **277,** 25266–25272
24. Dicker, F., Quitterer, U., Winstel, R., Honold, K., and Lohse, M. J. (1999) *Proc. Natl. Acad. Sci. U. S. A.* **96,** 5476–5481
25. Perroy, J., Adam, L., Qanbar, R., Chenier, S., and Bouvier, M. (2003) *EMBO J.* **22,** 3816–3824
26. Lefkowitz, R. J. (1998) *J. Biol. Chem.* **273,** 18677–18680
27. Bunemann, M., and Hosey, M. M. (1999) *J. Physiol. (Lond.)* **517,** 5–23
28. Kim, O. J., Gardner, B. R., Williams, D. B., Marinec, P. S., Cabrera, D. M., Peters, J. D., Mak, C. C., Kim, K. M., and Sibley, D. R. (2004) *J. Biol. Chem.* **279,** 7999–8010
29. Su, Y. F., Harden, T. K., and Perkins, J. P. (1980) *J. Biol. Chem.* **255,** 7410–7419
30. Chen, Z., Gaudreau, R., Le Gouill, C., Rola-Pleszczynski, M., and Stankova, J. (2004) *Mol. Pharmacol.* **66,** 377–386
31. Mukherjee, C., Caron, M. G., and Lefkowitz, R. J. (1975) *Proc. Natl. Acad. Sci. U. S. A.* **72,** 1945–1949
32. Tsao, P., and von Zastrow, M. (2000) *Curr. Opin. Neurobiol.* **10,** 365–369
33. Oakley, R. H., Laporte, S. A., Holt, J. A., Barak, L. S., and Caron, M. G. (2001) *J. Biol. Chem.* **276,** 19452–19460
34. Shenoy, S. K., and Lefkowitz, R. J. (2003) *Biochem. J.* **375,** 503–515
35. Tulipano, G., Stumm, R., Pfeiffer, M., Kreienkamp, H. J., Hollt, V., and Schulz, S. (2004) *J. Biol. Chem.* **279,** 21374–21382
36. Gray, J. A., Sheffler, D. J., Bhatnagar, A., Woods, J. A., Hufeisen, S. J., Benovic, J. L., and Roth, B. L. (2001) *Mol. Pharmacol.* **60,** 1020–1030
37. Clark, R. B., and Rich, T. C. (2003) *Mol. Pharmacol.* **64,** 1015–1017
38. Krupnick, J. G., Santini, F., Gagnon, A. W., Keen, J. H., and Benovic, J. L. (1997) *J. Biol. Chem.* **272,** 32507–32512
39. Cao, H., Thompson, H. M., Krueger, E. W., and McNiven, M. A. (2000) *J. Cell Sci.* **113,** 1993–2002
40. Adamus, G., Arendt, A., and Hargrave, P. A. (1991) *J. Neuroimmunol.* **34,** 89–97
41. Premont, R. T., Koch, W. J., Inglese, J., and Lefkowitz, R. J. (1994) *J. Biol. Chem.* **269,** 6832–6841
42. Bustin, S. A. (2000) *J. Mol. Endocrinol.* **25,** 169–193
43. Dumuis, A., Bouhelal, R., Sebben, M., Cory, R., and Bockaert, J. (1988) *Mol. Pharmacol.* **34,** 880–887
44. Oakley, R. H., Laporte, S. A., Holt, J. A., Barak, L. S., and Caron, M. G. (1999) *J. Biol. Chem.* **274,** 32248–32257
45. Lefkowitz, R. J., Pierce, K. L., and Luttrell, L. M. (2002) *Mol. Pharmacol.* **62,** 971–974
46. Willets, J. M., Nash, M. S., Challiss, R. A., and Nahorski, S. R. (2004) *J. Neurosci.* **24,** 4157–4162
47. Malecz, N., Bambino, T., Bencsik, M., and Nissenson, R. A. (1998) *Mol. Endocrinol.* **12,** 1846–1856
48. Iwata, K., Luo, J., Penn, R. B., and Benovic, J. L. (2005) *J. Biol. Chem.* **280,** 2197–2204
49. Penela, P., Ribas, C., and Mayor, F., Jr. (2003) *Cell. Signal.* **15,** 973–981
50. Pals-Rylaarsdam, R., Xu, Y., Witt-Enderby, P., Benovic, J. L., and Hosey, M. M. (1995) *J. Biol. Chem.* **270,** 29004–29011
51. Celver, J., Xu, M., Jin, W., Lowe, J., and Chavkin, C. (2004) *Mol. Pharmacol.* **65,** 528–537
52. Lamey, M., Thompson, M., Varghese, G., Chi, H., Sawzdargo, M., George, S. R., and O'Dowd, B. F. (2002) *J. Biol. Chem.* **277,** 9415–9421
53. Walker, J. K., Premont, R. T., Barak, L. S., Caron, M. G., and Shetzline, M. A. (1999) *J. Biol. Chem.* **274,** 31515–31523
54. Gray, J. A., Bhatnagar, A., Gurevich, V. V., and Roth, B. L. (2003) *Mol. Pharmacol.* **63,** 961–972
55. Paing, M. M., Stutts, A. B., Kohout, T. A., Lefkowitz, R. J., and Trejo, J. (2002) *J. Biol. Chem.* **277,** 1292–1300
56. Smyth, E. M., Austin, S. C., Reilly, M. P., and FitzGerald, G. A. (2000) *J. Biol. Chem.* **275,** 32037–32045
57. Vines, C. M., Revankar, C. M., Maestas, D. C., LaRusch, L. L., Cimino, D. F., Kohout, T. A., Lefkowitz, R. J., and Prossnitz, E. R. (2003) *J. Biol. Chem.* **278,** 41581–41584
58. van Koppen, C. J., and Kaiser, B. (2003) *Pharmacol. Ther.* **98,** 197–220
59. Holliday, N., Lam, C. W., Tough, I. R., and Cox, H. M. (2005) *Mol. Pharmacol.* **67,** 655–664
60. Shiina, T., Arai, K., Tanabe, S., Yoshida, N., Haga, T., Nagao, T., and Kurose, H. (2001) *J. Biol. Chem.* **276,** 33019–33026
61. Joubert, L., Hanson, B., Barthet, G., Sebben, M., Claeysen, S., Hong, W., Marin, P., Dumuis, A., and Bockaert, J. (2004) *J. Cell Sci.* **117,** 5367–5379
62. Gage, R. M., Matveeva, E. A., Whiteheart, S. W., and von Zastrow, M. (2005) *J. Biol. Chem.* **280,** 3305–3313
63. Bockaert, J., Fagni, L., Dumuis, A., and Marin, P. (2004) *Pharmacol. Ther.* **103,** 203–221
64. Lucas, G., Compan, V., Charnay, Y., Neve, R. L., Nestler, E. J., Bockaert, J., Barrot, M., and Debonnel, G. (2005) *Biol. Psychiatry* **57,** 918–925
65. Moser, P. C., Bergis, O. E., Jegham, S., Lochead, A., Duconseille, E., Terranova, J. P., Caille, D., Berque-Bestel, I., Lezoualc'h, F., Fischmeister, R., Dumuis, A., Bockaert, J., George, P., Soubrie, P., and Scatton, B. (2002) *J. Pharmacol. Exp. Ther.* **302,** 731–741

Uncoupling and Endocytosis of 5-Hydroxytryptamine 4 Receptors: DISTINCT MOLECULAR EVENTS WITH DIFFERENT GRK2 REQUIREMENTS

Gaël Barthet, Florence Gaven, Bérénice Framery, Katsuhiro Shinjo, Takaaki Nakamura, Sylvie Claeysen, Joël Bockaert and Aline Dumuis

Access the most updated version of this article at doi: 10.1074/jbc.M502272200

Alerts:
- When this article is cited
- When a correction for this article is posted

Click here to choose from all of JBC's e-mail alerts

Supplemental material:
http://www.jbc.org/content/suppl/2005/06/03/M502272200.DC1

This article cites 65 references, 45 of which can be accessed free at
http://www.jbc.org/content/280/30/27924.full.html#ref-list-1

Supplementary Table 1: Primers used for quantitative PCR. For each gene are indicated the Genbank accession number of the reference sequence used (Ref Seq), the nucleotide numbers in this sequence at which the primers start, and the sequences of forward and reverse primers.

cDNA	Ref Seq	Forward primer		Reverse primer	
m5-HT$_{4(a)}$	Y09587	m5-HT4(a)-1056F	TGGATCCACCCATGTACTAAGGT	m5-HT4(a)-1109R	GTGTATGGGCAATTTCTCCAGTT
m5-HT$_{4(b)}$	Y09585	m5-HT4(b) - 1028F	CTGTCCCCTGTTCAACCACAA	m5-HT4(b) - 1092R	CTCTCCCACTGGCCACCA
m5-HT$_{4(e)}$	Y09588	m5-HT4(e) - 1028F	CTGTCCCCTGTTCAACCACAA	m5-HT4(e) - 1086R	AACAGGTCTATTGCGGAAGAGC
m5-HT$_{4(f)}$	AJ011369	m5-HT4(e) - 987F	TGATGATGAGCGCTACAAAAGAC	m5-HT4(f) - 1066R	GACGGGAACAGGTCTTAGTACATG